Prochlorococcus rely on microbial interactions rather than on chlorotic resting stages to survive long-term stress

Dalit Roth-Rosenberg[1]#, Dikla Aharonovich[1]#, Tal Luzzatto-Knaan[1]#, Angela Vogts[2], Luca Zoccarato[3], Falk Eigemann[2], Noam Nago[1], Hans-Peter Grossart[3,4], Maren Voss[2] and Daniel Sher *[1]

[1] Department of Marine Biology, Leon H. Charney School of Marine Sciences, University of Haifa, 31905, Israel; [2] Leibniz-Institute for Baltic Sea Research, Seestrasse 15, D-18119 Warnemuende, Germany; [3] Department of Experimental Limnology, Leibniz-Institute of Freshwater Ecology and Inland Fisheries, Alte Fischerhuette 2, D-16775 Stechlin, Germany; [4]Potsdam University, Institute of Biochemistry and Biology, Maulbeeralle 2, D-14469 Potsdam, Germany

* Corresponding author: dsher@univ.haifa.ac.il

# These authors contributed equally to this study

Running title: Chlorosis and survival in *Prochlorococcus*

Abstract

Many microorganisms produce resting cells with low metabolic activity that allow them to survive prolonged nutrient or energy stress. We show that *Prochlorococcus*, the dominant phytoplankton lineage in large regions of the nutrient-poor ocean, cannot survive extended stress alone. In late stationary phase cultures, some cells retain metabolic activity (single-cell carbon and nitrogen uptake), but these axenic cultures do not re-grow when transferred into new media. However, when co-cultured with a heterotrophic bacterium, *Prochlorococcus* survived nutrient starvation for months. This dependence on heterotrophic bacteria is not limited to nutrient starvation - up to 10% of the *Prochlorococcus* cells in the oceans live under conditions of light starvation, surviving by utilizing organic compounds released by other microorganisms. We propose that reliance on co-occurring heterotrophic bacteria or on the organic compounds they produce, rather than the ability to survive extended starvation as resting cells, underlies the ecological success of *Prochlorococcus*.

Introduction

Not all microbial cells living in natural environments are equally active. In aquatic environments, up to 90% of the cells do not exhibit measurable metabolic activity ("vitality"), based on dyes (e.g. that assess electron transport) or on uptake assays with labeled substrates (1). Several possible and non-exclusive explanations have been proposed for this heterogeneity. First, inherent differences in activity between genetically-different organisms, e.g. due to variations in maximum growth rate or the ability to utilize the specific substrate tested. Second, cells might be at different physiological states, e.g. exponentially growing, starved or dying, and thus exhibiting different levels of metabolic activity (2, 3). Third, cells show stochastic fluctuations in their activity, due to noise in gene expression or regulatory networks (4). Finally, some organisms respond to environmental stress by producing resting stages or spores. Such cells often exhibit very low (or undetectable) metabolic activity, yet are viable, namely able to return to

49 an active state and reproduce when environmental conditions return to favorable (5). The presence of
50 such resting stages, together with a fluctuating activity at the single-cell level and the genetic variability
51 found within natural populations, are suggested to promote the survival of the population as a whole (2,
52 6).

53 Understanding the factors affecting the metabolic activity (vitality) of phytoplankton is of special
54 interest. These microbial primary producers perform about one-half of the photosynthesis on Earth,
55 providing energy through carbon fixation at the base of the aquatic ecosystem (7). As phytoplankton
56 grow, they take up elements such as nitrogen (N) and phosphorus (P) from the environment, potentially
57 leading to low nutrient concentrations that may constrain the growth of both the phytoplankton
58 themselves and co-occurring organisms (8, 9). Phytoplankton viability, including their ability to survive
59 under conditions of nutrient stress, has been extensively studied, especially for organisms that produce
60 massive blooms that emerge and decline rapidly (reviewed by (10-12)). For example, some bloom-
61 forming cyanobacteria such as *Aphanizomenon* species produce morphologically-distinct spores that
62 show very little photosynthetic activity, yet remain viable in the sediment for long periods of time,
63 providing the inoculum for the next growth season (13). In laboratory cultures of *Synechococcus*
64 *elegantus* PCC 7942 and *Synechocystis* PCC 6803, two unicellular freshwater cyanobacteria, nitrogen
65 starvation results in a programmed process where cells enter a resting stage, enabling them to survive
66 prolonged periods of stress (14, 15). As part of this process, cells degrade their photosynthetic
67 apparatus in a controlled manner, resulting in a loss of chlorophyll autofluorescence and culture
68 bleaching (a process termed chlorosis). However, the observation that chlorotic cells are viable resting
69 stages is not universal. Chlorotic cultures of *Microcystis aeruginosa* PCC 7806 were shown to contain a
70 small population of non-chlorotic cells with high chlorophyll auto-fluorescence (described throughout
71 this study as "high-fl"). Only these high-fl cells were suggested to revive after the re-addition of a
72 nitrogen source, while the low-fl cells are presumably dead (16). Chlorotic cells were also observed in

73 eukaryotic phytoplankton albeit it is not yet clear to what extent such cells remain viable as it may
74 depend on the specific organism and stress conditions (11, 17, 18).

75 *Prochlorococcus* is a pico-cyanobacterium that is extremely abundant in the oligotrophic oceans,
76 performing an estimated ~8.5% of global ocean photosynthesis (19). The carbon fixed by these
77 organisms, estimated to produce up to 75% of the daily photosynthetic carbon in the surface layer of
78 the Pacific subtropical gyre (20), can then be utilized by co-occurring heterotrophic bacteria.
79 *Prochlorococcus* cells in the oceans exhibit extremely high genetic diversity (21), and some of this
80 diversity has been linked with their ability to grow under conditions of extreme nutrient limitation (e.g.
81 (22, 23)). It has therefore been suggested that this genetic diversity enables *Prochlorococcus* as a group
82 to thrive across a wide variety of oceanic conditions (24). While the physiological and transcriptional
83 responses of multiple *Prochlorococcus* lineages to short-term nutrient starvation have been extensively
84 studied (e.g. (22, 25-29)), little is known about their ability to survive more than a few days under such
85 conditions. A study on the response of *Prochlorococcus* strains to extended darkness (i.e. C starvation)
86 has shown that these organisms can survive light starvation only for a limited time (30). In these
87 experiments, low-fl cell populations reminiscent of chlorotic cells in other cyanobacteria appear after
88 the light-starved cultures were re-exposed to light, regardless of whether these cultures could continue
89 growing (30). Our experiments were therefore designed to answer the following questions: i) Do
90 *Prochlorococcus* respond to long-term nutrient starvation by producing chlorotic cells? ii) If so, are such
91 cells metabolically active (vital) and are they able to reproduce and grow when stress conditions end
92 (viable)? iii) Can chlorotic *Prochlorococcus* cells be observed in nature? To address these questions, we
93 used fluorescence-activated cell sorting (FACS) to obtain distinct chlorotic sub-populations from axenic
94 and unialgal laboratory cultures of *Prochlorococcus* which were pre-incubated with isotopically-labelled
95 tracers for photosynthesis ($H^{13}CO_3$) and nutrient uptake ($^{15}NH_4^+$) and we visualized their activity using
96 Nanoscale Secondary Ion Mass Spectrometry (NanoSIMS). This method enabled us to measure

97 photosynthesis and N uptake at a single cell resolution by quantifying the change in isotopic ratios (31,
98 32). Our results show that while *Prochlorococcus* do undergo a chlorosis-like process, with some of the
99 chlorotic cells still photosynthesizing and taking up NH_4^+, the chlorotic cells are unable to re-grow and
100 thus do not represent resting stages. Instead, co-culture with heterotrophic bacteria in the lab and
101 mixotrophy in the ocean, two aspects of microbial interactions, enable *Prochlorococcus* to survive long-
102 term stress even without producing resting stages.
103

104 **Results and discussion**

105 **Emergence of chlorotic sub-populations in *Prochlorococcus* cultures**

106 As *Prochlorococcus* batch cultures reach stationary stage and start declining, the green color of the
107 cultures disappears, and sub-populations of cells emerge with lower chlorophyll autofluorescence that
108 can be identified by flow cytometry (Figure 1A, B). This phenomenon is observed in strains from all
109 major cultured ecotypes, as well as in a marine *Synechococcus*, strain WH8102 (Figure 1C). In the high-
110 light adapted strain *Prochlorococcus* MIT9312, lower chlorophyll populations emerged in batch cultures
111 that reached stationary stage due to both N and P limitation, although the timing of sub-population
112 emergence and the forward light scatter and chlorophyll autofluorescence (analyzed by flow cytometry)
113 were different under the two nutrient stresses (Supplementary Fig. 1A, B). Cells with lower chlorophyll
114 autofluorescence also appeared in populations of another strain, the low-light adapted MIT9313, when
115 these cultures were inhibited in a co-culture with high cell densities of the heterotrophic bacterium
116 *Alteromonas* HOT1A3 (Supplementary Fig. 1C, D (33)). Thus, the emergence of populations of cells with
117 lower chlorophyll autofluorescence under a variety of stress conditions is a pervasive phenomenon
118 across marine pico-cyanobacteria. We focused our experiments aiming to better characterize this
119 phenomenon on *Prochlorococcus* strain MIT9313, as the response to stress in this strain has been
120 extensively studied (e.g. (22, 26, 27, 33-35)). Additionally, in this strain, three clearly separate sub-

121 populations can be observed when cultured in Pro99 media, facilitating the sorting and subsequent

122 nanoSIMS analyses (Figure 1B, referred to throughout the study as high-, mid- and low-fl populations).

123

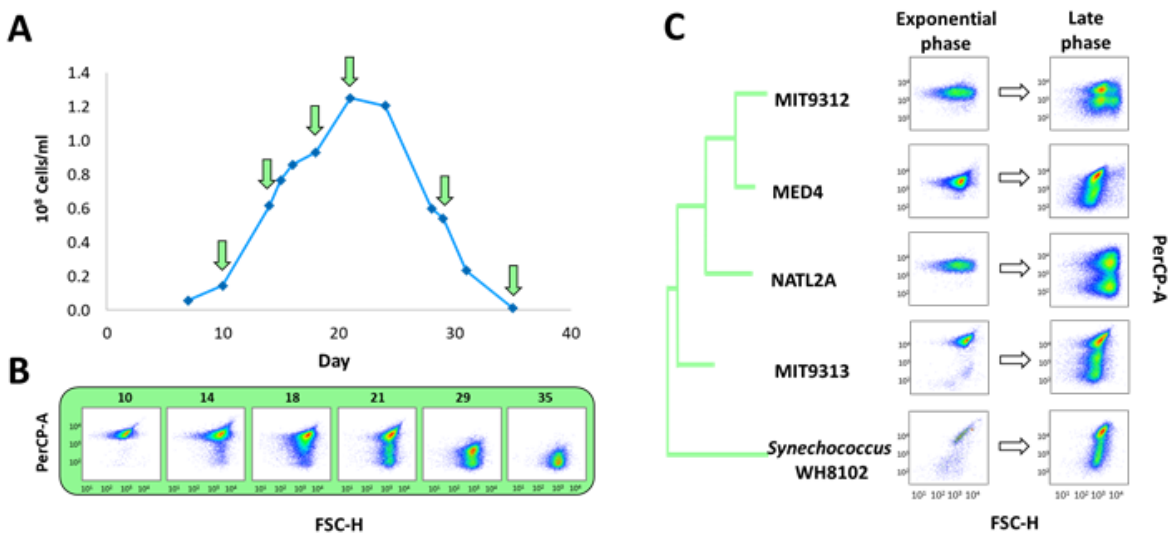

Figure 1. Emergence of chlorotic sub-populations in *Prochlorococcus* batch cultures as measured by flow cytometry. A) A representative growth curve of an axenic culture of MIT9313, grown in Pro99. The arrows mark the days shown in panel B. B) Flow cytometry scattergrams at the marked time-points from the MIT9313 culture. The x-axis is Forward Scatter (FSC, a proxy for cell size) and the y-axis is the chlorophyll autofluorescence of the cells (Per-CP). The emergence of chlorotic sub-population observed from the late exponential phase (Day 18). C) Chlorotic sub-population observed in ageing batch cultures of *Prochlorococcus*, belonging to different ecotypes: High-Light adapted MED4 (HLI), MIT9312 (HLII) and Low-Light adapted NATL2A (LLI) and MIT9313 (LLIV). In all strains, the chlorotic cells begin to emerge at late growth stage, becoming dominant in declining cultures, while in the exponential phase only one population can be observed. Additional growth curves for this strain and for others, including replicate standard deviations, as shown in Figures 3 and 4 and in

supplementary figures 1, 3, and 6-9.

124

125 **Assessing the metabolic activity of sorted chlorotic sub-populations**

126 We next asked whether the high, mid- and low-fl populations differ in their vitality, measured here as
127 their photosynthesis and nutrient uptake rates (incorporation of $H^{13}CO_3^-$ and $^{15}NH_4^+$, respectively). The
128 uptake ratio of labeled versus unlabeled nutrients were then used to calculate the metabolic activity of
129 the sorted cells (Table 1). As shown in Figure 2 and Table 1, the mean uptake of both $H^{13}CO_3^-$ and $^{15}NH_4^+$
130 was highest in the high-fl population, followed by the mid and low-fl populations, with the latter
131 population indistinguishable from the control, i.e. glutaraldehyde-killed cells. We have repeated the
132 entire workflow in an independent experiment, and the results are very similar (Supplementary Fig. 2,
133 Table 1). These results are reminiscent of observations in several eukaryotic phytoplankton (18).

134

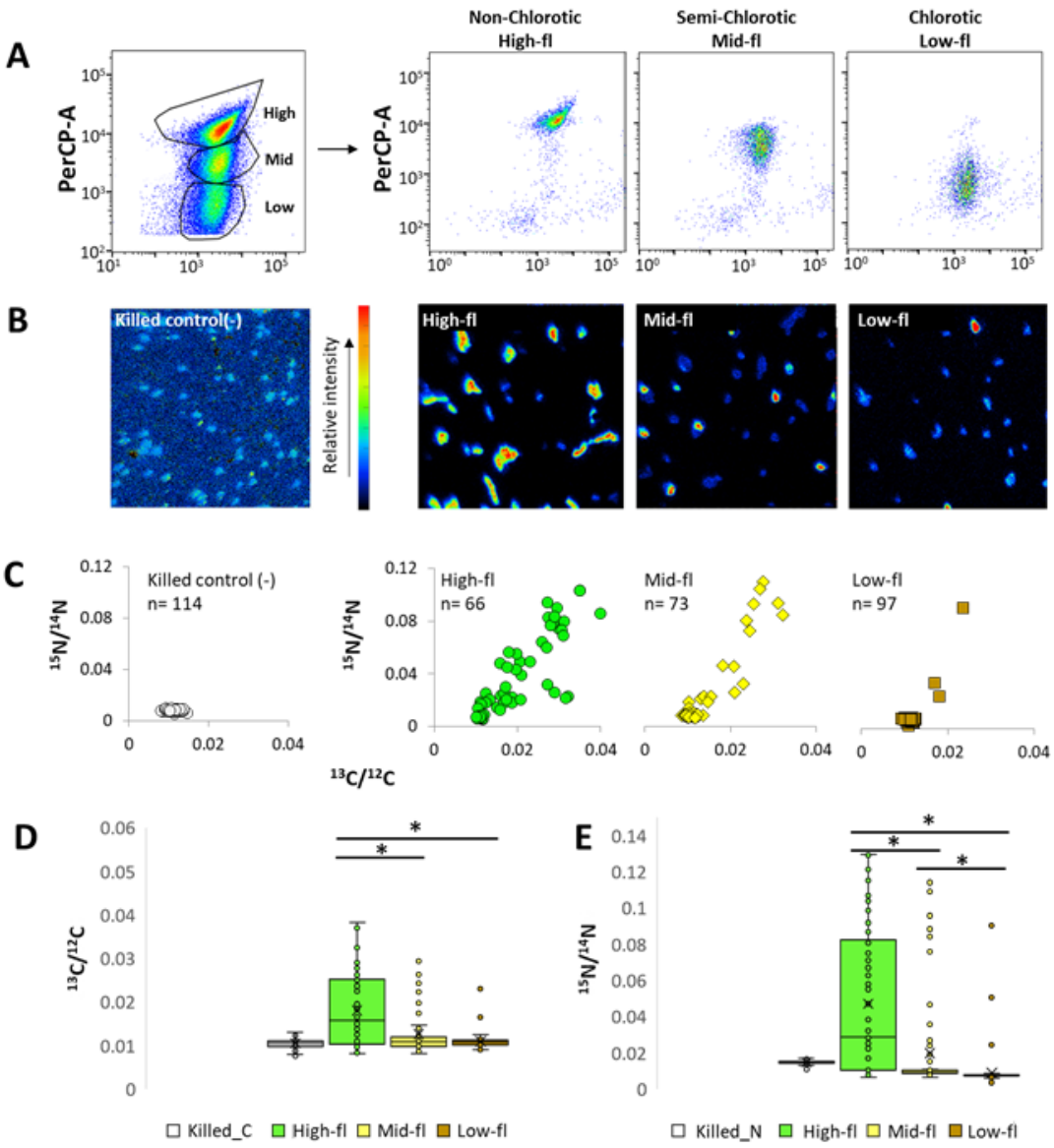

Figure 2. Metabolic activity of sorted sub-populations by NanoSIMS A) Flow cytometry scatterplots before and after sorting of three distinct sub-populations (high, mid and low-fl) of an aging *Prochlorococcus* MIT9313 culture, detected by flow cytometry. The cultures were grown for 30 days in Pro99 and labeled with $H^{13}CO_3^-$ and $^{15}NH_4^+$ for 18h. B) NanoSIMS images of $^{15}N/^{12}C$ analysis of killed cells (negative control) and high, mid and low-fl cells after sorting. C) Scatterplot of $^{13}C/^{12}C$ and $^{15}N/^{14}N$ ratios obtained from NanoSIMS analysis of each sub-population. D, E) Boxplots of the $^{13}C/^{12}C$ and $^{15}N/^{14}N$

enrichment in each sub-population. Lines represent the median, X represents the mean, box borders are 1st quartiles and whiskers represent the full range.

135

Strain and growth stage	Sub-population	Illumination	V^C (fg cell^{-1} day^{-1})	V^N (fg cell^{-1} day^{-1})
Batch culture				
MIT9313, exponential growth*	High	Constant light 27µE	12.92 ± 11.93	2.74 ± 2.43
MIT9313, old cultures **	High	Constant light 27µE	2.67-2.77 ± 2.89-3.57	0.62-0.69 ± 0.54-0.63
	Mid		0.75-0.79 ± 1.73-1.78	0.25-0.32 ± 0.42-0.35
	Low		0.09-0.14 ± 0.52-0.67	0.08-0.14 ± 0.15-0.12
MIT9313, old culture***	High	Photo-period 12:12 L/D, 27µE	1.01 ± 2.67	0.32 ± 0.33
	Mid		0.48 ± 2.47	0.20 ± 0.20
	Low		0.13 ± 0.31	0.14 ± 0.11
Natural samples				
115m	High	Natural cycle approximately 14:10 L/D,	1.04 ± 0.6	1.17 ± 0.20
115m	Low		1.14 ± 0.69	1.15 ± 0.38
125m	High		1.21 ± 0.89	1.28 ± 0.21

	2-5 µE

136

137 **Table 1: Calculated mean C and N uptake rates from the experiments performed with *Prochlorococcus***
138 **MIT9313 and natural samples.** The means and standard deviation were calculated from the uptake
139 rates values of single cells in each experiment.
140 *The results for MIT9313 exponential growth refers to the experiment presented in Supplementary Fig.
141 4.
142 **The results for old MIT9313 cultures under constant light refer to the two experiments presented in
143 Fig. 2 and Supplementary Fig. 2.
144 *** The results for Old MIT9313 cultures under L/D refer to the experiment presented in Supplementary
145 Fig. 3. The experiment was sampled after a longer period due to slower growth under a light-dark cycle
146 compared with constant light (Supplementary Fig 3A).
147 The mean uptake rates for glutaraldehyde killed cells (control) were 0.06±0.15 fg cell-1 day-1 for C and
148 0.18±0.02 fg cell-1 day-1 for N, and most likely depict the absorption of the label by non-specific binding
149 or diffusion.
150

151 Within each of the populations, cell-cell heterogeneity was observed in both ^{13}C and ^{15}N uptake
152 (Fig. 2, Supplementary Fig. 2). Within all of the populations (including the high-fl), some cells were
153 inactive, and this could not be explained by the limited purity of the FACS-sorting procedure
154 (Supplementary Tables 1, 2). The coefficients of variation in C and N uptake rates were within the range
155 shown for other organisms, or higher (Supplementary Table 3 (32, 36)). Similar levels of heterogeneity
156 (primarily in N uptake) were also seen in cells grown under a 12:12 light-dark cycle, where the
157 *Prochlorococcus* cell-cycle follows a diel rhythm, suggesting that this heterogeneity is not due to
158 different stages of the cell cycle or the diel cycle (Supplementary Table 3, Supplementary Fig. 3). Cell-cell

159 heterogeneity was also observed in cells from an exponentially-growing, nutrient-replete culture
160 (Supplementary Figure 4, Table 3), suggesting that this heterogeneity is not exclusively limited to ageing
161 or stressed cells. This is in accordance with studies assessing the vitality of *Prochlorococcus* cells using
162 various dyes, which consistently show that a significant fraction of the cells in laboratory cultures are
163 inactive or potentially dead (37, 38).

164 In addition to differing in their chlorophyll autofluorescence and metabolic activity, the high-, mid-
165 and low-fl cell populations also differ by their forward and side light scatter properties, which are
166 related to cell size and (in larger cells) morphological complexity (Supplementary Fig 5A, B). In
167 agreement with these observations, cells sorted from the high-fl population and observed by SEM
168 (Scanning Electron Microscopy) were 20-30% larger than those from the mid- and low-fl populations
169 (Sup Fig 2C, D).

170

171 **Evaluating the viability of sub-populations**

172 To determine whether the low-fl *Prochlorococcus* MIT9313 cells are viable resting stages, we tested the
173 ability of cells from MIT9313 cultured in Pro99 media to grow upon transfer to new growth media at
174 different times during exponential growth and upon culture decline. As shown in Figure 3A, only cells
175 from cultures where the high-fl cells were dominant could grow when transferred to new growth media.
176 No growth was observed upon transfer of cells from stationary or declining cultures where no high-fl
177 cells were observed. Intriguingly, the presence of high-fl cells was not enough to ensure culture growth
178 (e.g. day 34 in Figure 3A). This is consistent with a previous study showing that cells belonging to a
179 different *Prochlorococcus* strain, MED4, that were incubated for three days in the dark, were unable to
180 resume growth after return to light despite showing no clear difference in the chlorophyll
181 autofluorescence (30). The probability of growth after transfer did not depend on the number of

182 transferred cells (39), with as many as 2.5×10^7 cells/ml failing to grow after transfer during culture
183 decline (cells at ~1/10 of this density grew after being transferred during exponential stage). Thus, non-
184 chlorotic cells (defined as being within the range of chlorophyll autofluorescence exhibited by
185 exponentially-growing cells) are not necessarily viable.

186 One problem with performing experiments in Pro99, which is commonly used to culture
187 *Prochlorococcus*, is that the conditions causing cells to reach stationary stage are not always clear (e.g.
188 (40). We therefore repeated these experiments under conditions where entry into stationary phase is
189 induced by N or P starvation (Figure 3B, Supplementary Fig 6, (41)). When entry into stationary stage
190 was induced by N or P starvation, chlorotic cells appeared much faster, and the cultures became non-
191 viable much earlier – essentially immediately after the cessation of exponential growth. Similar results
192 were obtained with a different strain of *Prochlorococcus*, MIT9312 (Supplementary Figure 7). However,
193 a marine *Synechococcus* (strain WH8102) behaved differently, surviving N starvation much longer and
194 being able to re-grow in nutrient replete media long after the culture started declining, and when
195 essentially all cells were chlorotic (Supplementary Figure 8). This is reminiscent of the ability of
196 (presumably axenic) cultures of two freshwater cyanobacteria, *Synechococcus* PCC 7942 and
197 *Synechocystis* PCC 6803, to revive after extended N starvation (14, 15).

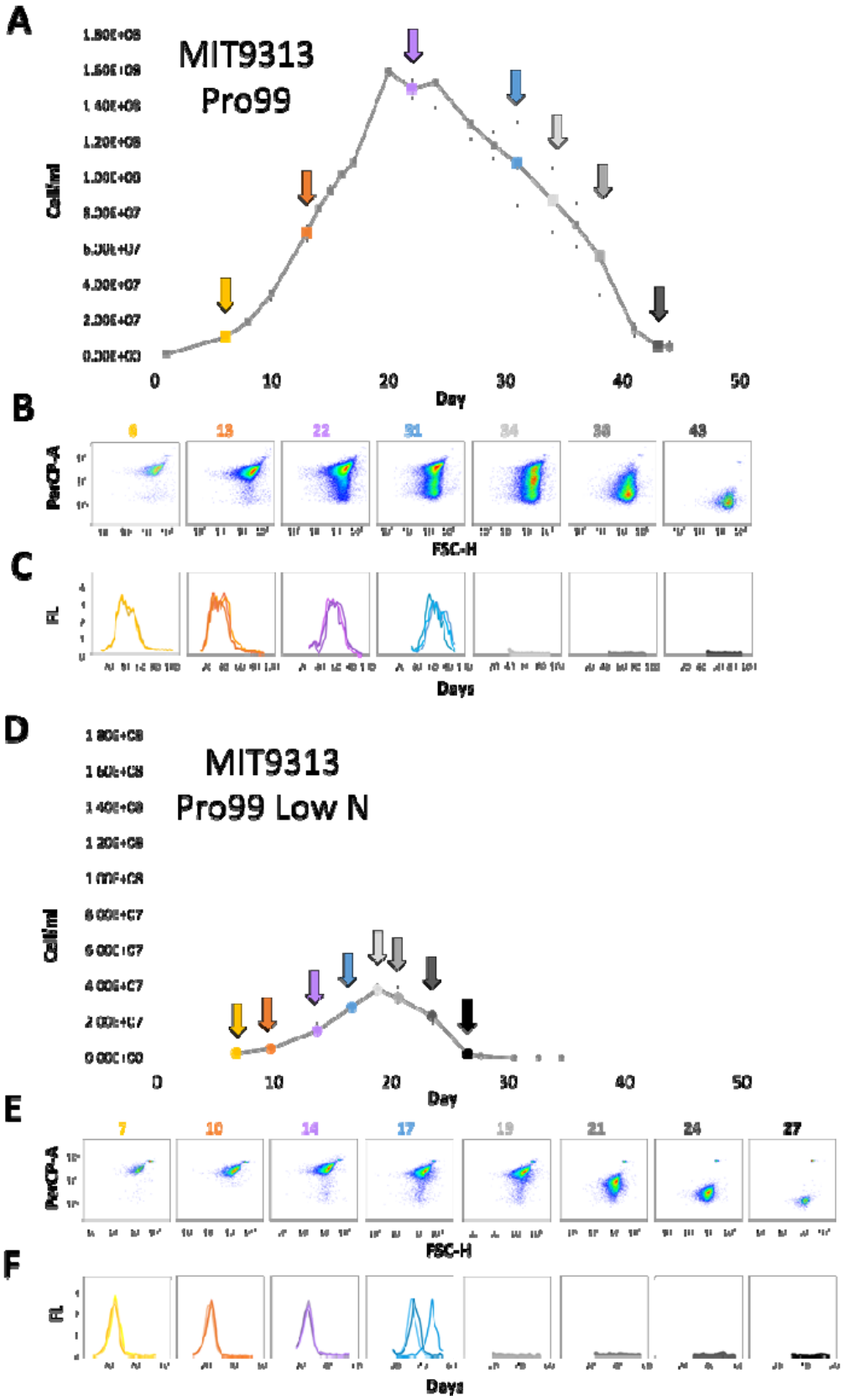
A
MIT9313
Pro99
Cell/ml
Day
B
PerCP-A
FSC-H
C
FL
Days
D
MIT9313
Pro99 Low N
Cell/ml
Day
E
PerCP-A
FSC-H
F
FL
Days

Figure 3: Time-dependent changes in viability of cells transferred into fresh media at different life cycle stages of a batch culture for MIT9313 in Pro99 (A-C) and when stationary stage is induced by N starvation (D-F). A, D) Growth curves of a MIT9313 culture, in Pro99 media commonly used for *Prochlorococcus* culturing (A) and under conditions where stationary stage is induced by nitrogen starvation (panel D, 2:1 N/P ratio in the growth media, (41)). Colored circles indicate the times point at which triplicate 1ml samples were transferred into 20 ml fresh media. B, E) Flow cytometry scatterplots of the culture shown in panels A and D. Note that, under conditions of N starvation, the cultures shift rapidly from being comprised primarily of high-fl cells (day 19 in panel E, early stationary phase) to mainly mid-fl cells, with essentially no high-fl cells (day 21 in panel E). C, F) Growth curves of cells being transferred at different times to new, nutrient-replete media (assessed via bulk culture fluorescence). In these plots, each line shows a replicate culture. Cells could not re-grow when transferred after more than 31 days in Pro99 and 17 days of nitrogen starvation. This suggests that, in this strain, high-fl cells are not necessarily viable.

198

199

200 The inability of *Prochlorococcus* strains to survive long-term nutrient starvation was surprising,
201 and we therefore hypothesized that their survival would be enhanced by interactions with co-occurring
202 heterotrophic bacteria. Indeed, when co-cultured with a heterotrophic bacterium, *Alteromonas* HOT1A3
203 (33, 42), *Prochlorococcus* strains representing all major cultured ecotypes were able to re-grow after 60
204 days of N and P stress, whereas all axenic strains failed to do so (Figure 4, supplementary Figure 9).
205 Interestingly, strain MIT9313, which was initially inhibited by this *Alteromonas* strain (Figure 4A, (33,
206 43)), was also able to survive long-term starvation in co-culture, suggesting that fundamentally different
207 interactions occur during exponential growth compared to long-term, presumably nutrient-limited

growth. These results are consistent with the ability of heterotrophic bacteria to extend the survival time of different *Prochlorococcus* strains under conditions of constant darkness (albeit for only several days, (30)) and with the ability of different heterotrophic bacteria to support the long-term viability of batch cultures of *Synechococcus* WH7803 (44). We observed similar results when *Prochlroococcus* cultures were transferred from nutrient-replete media into sterile sea water with no added nutrients (Supplementary Figure 10). This suggests that the ability of the heterotrophs to support *Prochlorococcus* survival is due to nutrient remineralization rather than to the detoxification of potential waste products, although a potential role for de-toxification cannot be ruled out (Christie-Oleza et al. 2017).

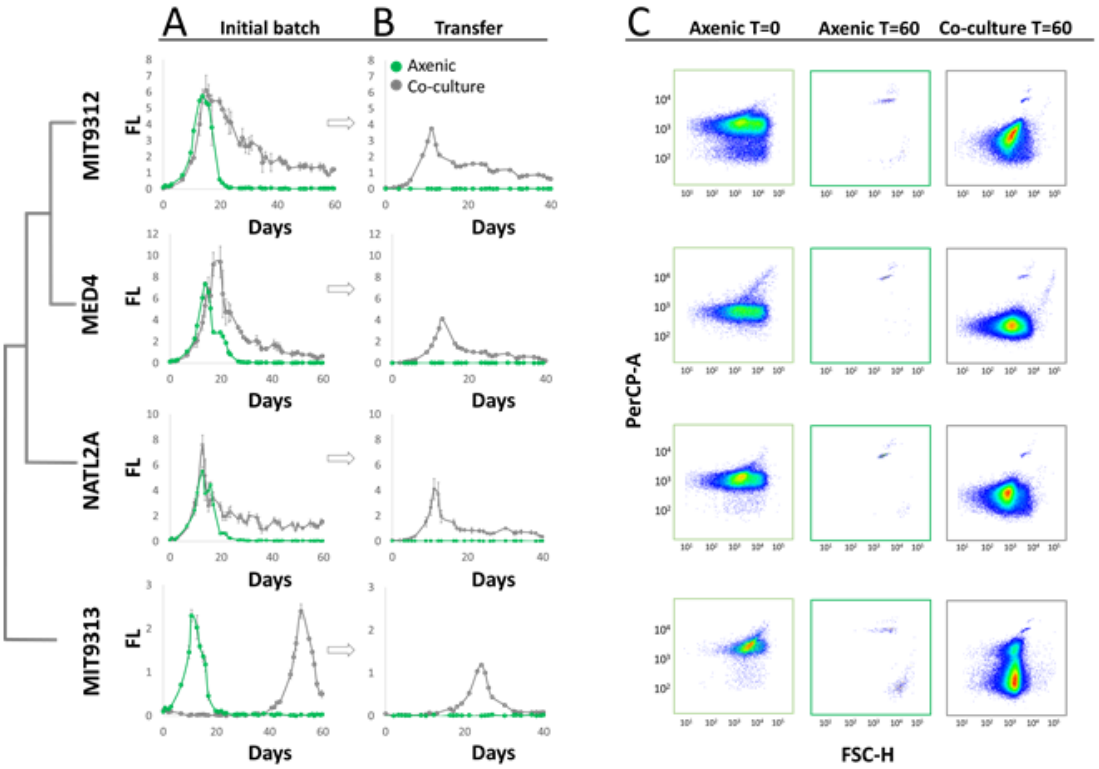

Figure 4: Co-culture with a heterotrophic bacterium, *Alteromonas* HOT1A3, enables multiple *Prochlorococcus* strains to survive long-term N starvation. A) 10^6 axenic *Prochlorococcus* cells ml^{-1} from different strains were incubated alone (green line) or with the addition of 10^7 *Alteromonas* HOT1A3 cells

ml^{-1} in low-N media (grey line). Bulk culture fluorescence was recorded as a proxy for cell growth, and 1ml from each culture was transferred into 25ml fresh Pro99 media after 60 days. Panel B) The transferred cultures were recorded for additional 40 days. Error bars are standard deviation from triplicate cultures. The late growth of MIT9313 in co-culture is the "delayed growth" phenotype described in (33, 43). C) Flow cytometry scattergrams of the cultures shown in panel A. Co-culture with *Alteromonas* increases the number of *Prochlorococcus* cells seen by flow cytometry, suggesting a reduction in the magnitude of mortality (cell lysis). A decrease in per-cell chlorophyll autofluorescence is still seen.

216

217 **Exploring the metabolic activity of naturally occurring sub-populations of *Prochlorococcus* at different**
218 **depths in the eastern Mediterranean**

219 While chlorotic cells consistently emerge under nutrient starvation in all tested *Prochlorococcus* strains
220 (Fig 1), growth conditions in laboratory cultures greatly differ from those in the oligotrophic sea. For
221 example, in the experiments described above, where the immediate cause for cessation of growth is N
222 or P starvation (Figure 3, Supplementary Figures 6-10), cell densities and nutrient concentrations are still
223 orders of magnitude higher in the lab than in the nutrient-poor ocean. Under these conditions, pH might
224 vary significantly, and potentially toxic by-products of cell metabolism can accumulate (40, 44). Indeed,
225 little is known about the prevalence of chlorosis under natural conditions for phytoplankton in general,
226 which include variability in light intensity, nutrient concentrations etc. Thus, we wondered whether
227 chlorotic *Prochlorococcus* cells (defined as low-fl and low C and N uptake) can be identified also in
228 nature. We focused on the deep euphotic zone (100-140m, above the nutricline) where both inorganic
229 nutrient concentrations and light availability are low. At this depth, "double" *Prochlorococcus*
230 populations, differing by their chlorophyll auto-fluorescence, have repeatedly been observed (e.g. (45,

231 46)). Previously, these double populations have been shown to contain genetically-different cells
232 belonging to the High-Light adapted (HL, low chlorophyll) and Low-Light adapted (LL, high chlorophyll)
233 clades (46), However, a recent study using genetic tools suggested that each of the double populations
234 consists of both HL and LL cells, implying that phenotypic heterogeneity (acclimation) can also
235 contribute to this phenomenon (47). We therefore asked whether the double population could also be
236 due to the presence of chlorotic cells, a process that could occur if, for example, LL cells were mixed
237 above the nutricline, became exposed to nutrient starvation, and subsequently underwent chlorosis. To
238 test this hypothesis, we characterized the *Prochlorococcus* population structure and single-cell activity
239 (carbon fixation and NH_4^+ uptake) during late summer in the ultra-oligotrophic Eastern Mediterranean
240 Sea (Figure 5A, B). At the time of sampling, the water column was highly stratified and nutrients were
241 depleted down to around 130 m, with a peak in NH_4^+ concentrations slightly above the nutricline (15nM
242 at 115m and 125m, Fig. 5B). *Prochlorococcus* were the numerically dominant phytoplankton (Fig 5C),
243 exhibiting a double population at 115 m, but not at samples collected above or below this depth (Fig 5E).
244 Amplicon sequencing of the Internal Transcribed Spacer between the 16S and 23S genes (ITS, (47, 48))
245 revealed that between ~100-137 m LL cells (belonging primarily to the LL-I and LL-IV clades) gradually
246 replace the HL cells. This is consistent with previous studies (e.g. (47, 49)) but contrasting with the sharp
247 delineation between the flow-cytometrically defined high-chlorophyll and low-chlorophyll
248 *Prochlorococcus* populations (Fig. 5E, (47)).

249 Mean $H^{13}CO_3^-$ and $^{15}NH_4^+$ uptake rates for the majority of the cells sorted from each of the
250 double *Prochlorococcus* populations at 115m depth were not statistically different, nor were they
251 different from cells collected at greater water depths (Figure 5. F, G, Kruskal-Wallis test, p=0.7 for C and
252 p=0.07 for N). Essentially all of the cells from the Eastern Mediterranean were active, although we did
253 observe some cells with lower C and N uptake rates in the low-fl population at 115m depth (6/45 cells,
254 Figure 5F). This contrasts with the observation from our lab experiments, where inactive cells were

255 observed in all populations, and formed the majority of the cells in the chlorotic (mid- and low-fl)
256 populations. The observation that essentially all of the *Prochlorococcus* cells in natural samples are
257 active is consistent with a similar study in the North Pacific (32).

258 At a depth of 115 m, light intensity was low (5-6 μE during the afternoon), potentially enough to
259 support the growth of some LL strains but not sufficient for active growth under laboratory conditions of
260 most HL strains, including those that are present based on the ITS sequences (50). However, previous
261 studies based on cell cycle analysis and on ^{14}C incorporation into divinyl-chlorophyll a have suggested
262 that, even at this depth, *Prochlorococcus* cells divide every 4-7 days (51-54). The C uptake rates
263 observed in the cells from 115 and 137 m (~1 fg $cell^{-1}$ day^{-1}, Table 1) were well below the rate required to
264 support this division rate, even though the experiment was performed around midday when light
265 penetration was at its maximum. Additionally, unlike the laboratory cultures, in which C incorporation
266 rates were 3-6 times higher than N-incorporation rates, in our samples from the Mediterranean Sea the
267 measured C:N uptake ratio was about 1. Thus, a "deficit" exists in the C budget of *Prochlorococcus* at
268 these depths, suggesting that a significant part of the carbon needed for *Prochlorococcus* cell growth
269 was not fixed by the cells through photosynthesis, but rather came from the utilization of dissolved
270 organic C from other sources i.e. through mixotrophy (see below).

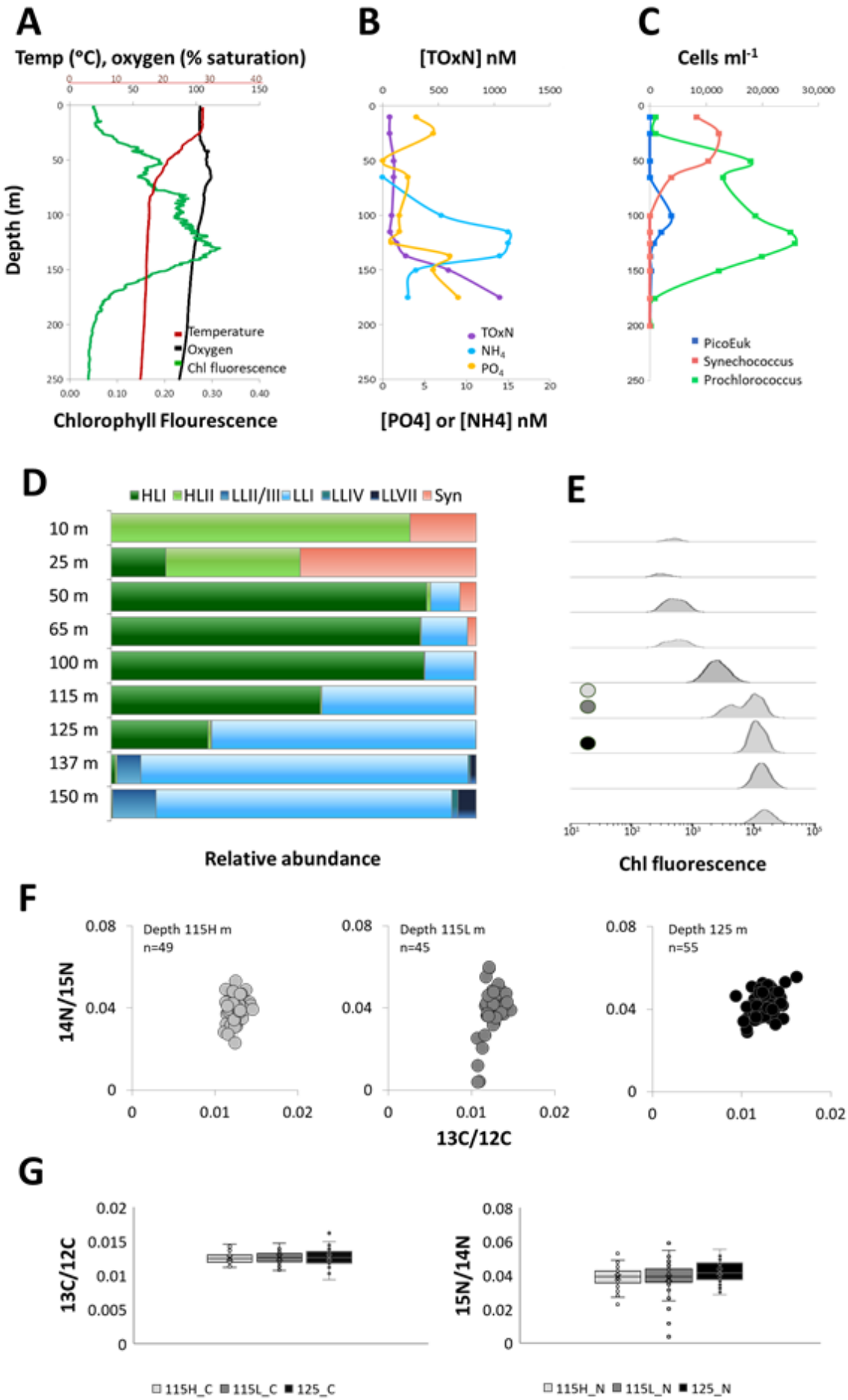
A
Temp (°C), oxygen (% saturation)
Depth (m)
Temperature
Oxygen
Chl fluorescence
Chlorophyll Flourescence
B
[TOxN] nM
TOxN
NH4
PO4
[PO4] or [NH4] nM
C
Cells ml-1
PicoEuk
Synechococcus
Prochlorococcus
D
HLI HLII LLII/III LLI LLIV LLVII Syn
10 m
25 m
50 m
65 m
100 m
115 m
125 m
137 m
150 m
Relative abundance
E
Chl fluorescence
F
Depth 115H m
n=49
Depth 115L m
n=45
Depth 125 m
n=55
14N/15N
13C/12C
G
13C/12C
115H_C 115L_C 125_C
15N/14N
115H_N 115L_N 125_N

Figure 5: Nutrient uptake of naturally occurring *Prochlorococcus* populations at the Eastern Mediterranean Sea. A-C) Oceanic parameters at the sampling site: Temperature, Oxygen and Chlorophyll (A); Nutrient concentration (TOxN refers to total oxidized nitrogen, NO_2+NO_3) (B); Cell counts by flow cytometry (C). D) Relative abundance of different *Prochlorococcus* clades across the water column, determined by ITS sequencing. E) Histograms of chlorophyll autofluorescence, analyzed from flow cytometry of picoplankton throughout the water column. Note the double population at 115m. The circles represent the populations sorted and analyzed by nanoSIMS. F) Scatterplot of $^{13}C/^{12}C$ and $^{15}N/^{14}N$ ratios obtained from NanoSIMS analysis of each sorted sub-population from 115m and the single population from 125m. G) Boxplots of the $^{13}C/^{12}C$ and $^{15}N/^{14}N$ enrichment in each sub-population. Lines represent the median, X represents the mean, box borders are 1st quartiles and whiskers represent the full range. The three populations did not statistically differ (Kruskal-Wallis test).

271

272 **Stress survival in pico-cyanobacteria: why is *Prochlorococcus* different?**

273 In this study, we demonstrate that phenotypic heterogeneity between clonal *Prochlorococcus* cells
274 occurs at multiple "scales". In exponentially growing axenic laboratory cultures of two strains, MIT9313
275 and MED4, C and N uptake rates differ significantly between individual cells (summarized in
276 Supplementary Table 3). This variation is independent of genetic variability, and is observed to some
277 extent in natural populations, suggesting this is a common attribute to all *Prochlorococcus* cells.
278 Additionally, as axenic cultures become stressed, a larger phenotypic change occurs as cells lose their
279 chlorophyll auto-fluorescence and become chlorotic. Under these experimental conditions, most cells
280 are inactive (primarily in the low-fl population, as measured in strain MIT9313), although, we cannot
281 rule out that even low-fl cells still retain a residual level of activity not detectable by the used methods.

282 Some cells from the chlorotic populations nevertheless retain at least part of their photosynthetic
283 capacity, and indeed can fix carbon and take up NH_4. Yet, in our experiments, they do not re-grow when
284 condition become more favorable. In *Synechococcus elegantus* PCC 7942, chlorotic cultures retain
285 approximately 0.01% of their photosynthetic activity, as well as a residual level of protein translation,
286 although it remains unclear whether this is a process shared by all cells in the culture or whether this
287 activity is only due to a small subset of more active cells (14). The clear difference between the ability of
288 axenic *Synechococcus elegantus* PCC 7942 and *Synechocystis* PCC6803 to survive long-term N starvation,
289 and the inability of axenic *Prochlorococcus* cultures to do so, suggests an inherent difference in the
290 physiology and genomic functional capacity between these unicellular cyanobacteria.

291 Entry into chlorosis in *Synechocystis* is a regulated process that involves the organized degradation of
292 the phycobilisomes in parallel with an increase in the storage products glycogen and
293 polyhydroxybutyrate (PHB) (15). The photosynthesis apparatus of *Prochlorococcus* is different from that
294 of other cyanobacteria, using unique chlorophyll a2/b2 binding proteins rather than phycobilisomes
295 (55), and indeed they lack orthologs of the nblA gene required for phycobilisome degradation during
296 chlorosis (15). Additionally, while *Prochlorococcus* likely use glycogen as a C storage pool (56), they lack
297 the phaA-C and phaE genes required for PHB biosynthesis and which are induced in *Synechocystis* PCC
298 6803 under chlorosis (although these genes are not required for revival from chlorosis (15)). Taken
299 together, these differences suggest that *Prochlorococcus* lack the genetic toolkit employed by
300 *Synechocystis* PCC6803 and *Synechococcus elegantus* PCC7942 to enter into a resting stage. However,
301 we note that *Synechococcus* WH8102 also lacks the gene nblA gene, yet can survive N starvation much
302 longer in axenic culture than the tested *Prochlorococcus* strains can (Sup Fig 8). This suggests that
303 additional molecular mechanisms besides nblA-mediated degradation of the phycobilisomes are
304 important for long-term survival of nutrient starvation in these organisms.

305 If *Prochlorococcus* are indeed incapable of producing resting stages in response to nutrient or light
306 starvation, what are the evolutionary drivers of this phenotype, and what are the consequences for the
307 dynamics of *Prochlorococcus* populations in the ocean? While the open oligotrophic ocean is often
308 considered a relatively stable environment, nutrient concentrations do fluctuate (8), and phytoplankton
309 (including *Prochlorococcus*) inhabiting these waters show multiple signs of nutrient stress (57). Many of
310 the microbes that live in such environments comprising a large fraction of the surface ocean have small,
311 highly streamlined genomes (58) and this has been suggested to be an adaptation to low nutrient
312 concentrations (24, 58, 59) . Therefore, it is possible that the lack of resting stages is a result of this
313 genome streamlining (the genomes of *Synechococcus elegantus* PCC7942 and *Synechocystis* PCC6803
314 are ~3.2mbp and ~4mbp with their plasmids, respectively, compared to ~1.4-2.5 mbp for
315 *Prochlorococccus* strains).

316

317 **Surviving nutrient stress "with a little help from my friends".**

318 Despite the clear effect of nutrient stress on *Prochlorococcus* in axenic laboratory culture, manifesting in
319 chlorosis and reduction of vitality, we observed relatively few less-active (potentially chlorotic)
320 *Prochlorococcus* cells in the deep euphotic zone of the Eastern Mediterranean (approximately 5% of the
321 population at 115 m, Figure 5F). It is possible that cell stress and chlorosis change as a function of the
322 diel cycle, and indeed previous studies have suggested *Prochlorococcus* cell mortality increases during
323 the night (20, 60). As the sampling of natural population in the Eastern Mediterranean Sea took place
324 during the day (~12:00-16:00) we cannot exclude this hypothesis. Alternatively, less-active or chlorotic
325 cells may be removed by selecting grazing (ref*). Finally, the ability of *Prochlorococcus* to thrive under
326 conditions of extreme nutrient limitation is often explained by their small cell size (increasing their
327 biomass-specific diffusion), their generally low nutrient requirements, and their specific metabolic

328 strategies to minimize the per-cell elemental quotas (61-63). However, these mechanisms appear not to
329 work in axenic laboratory cultures, and thus we propose that interactions with co-occurring
330 microorganisms, e.g. through the recycling of inorganic nutrients or the exchange of organic
331 compounds, enable *Prochlorococcus* to survive when nutrient-saving mechanisms are not sufficient, as
332 suggested for its close relative *Synechococcus* (44). Indeed, the observation that *Prochlorococcus* can
333 compete with heterotrophic bacteria for amino acids (64), carbohydrates (65) and perhaps DMSP (66,
334 67) suggests that the utilization of organic molecules by the phototrophic *Prochlorococcus* (mixotrophy)
335 is prevalent and important in natural communities. This is supported by genomic analyses (68, 69). The
336 importance of mixotrophy is not limited to organic forms of N or P, however: based on the field data
337 shown in Figure 5, and as shown in laboratory cultures by Coe and coworkers (30), mixotrophy in
338 *Prochlorococcus* might be important also during light starvation. To determine the potential magnitude
339 of this effect, we calculated the fraction of the *Prochlorococcus* cells in the north Atlantic and Pacific
340 gyres (Hawaii and Bermuda time series study sites, respectively (49)) that are found under conditions
341 where the average integrated illumination is not enough to support their growth under laboratory
342 conditions (50). As shown in Figure 6, an average of ~8-10% of the *Prochlorococcus* cells are likely light-
343 starved during stratified periods, including the vast majority of LL adapted ecotypes (see supplementary
344 text for more details). Notably, cell-specific amino acid uptake rates of *Prochlorococcus* from the
345 southern Atlantic Ocean increase with depth, and high-fl cells take up more than low-fl cells, although to
346 what extent this supports the C and N needs of the cells is unknown (64).

347 Regardless of the specific forms of dissolved organic carbon being utilized by the cells, the lack of any
348 observed mechanism for the production of resting stages by *Prochlorococcus* may be considered
349 another manifestation of the "Black Queen Hypothesis", which states that microorganisms "outsource"
350 essential survival mechanisms such as detoxification of reactive oxygen species to the surrounding
351 microbial community (70). These forms of microbial interactions likely affect the distribution and activity

352 of *Prochlorococcus* on a global scale. The increased survival of *Prochlorococcus* under harsh conditions,
353 supported by its associated heterotrophic bacteria, may enable it to remain active at the single cell level
354 even during long periods of unfavorable conditions (71, 72). Thus, the tight interactions between
355 *Prochlorcoccus* and its bacterial "supporters" likely affects photosynthesis and carbon cycling at the base
356 of the aquatic foodweb, with potentially profound implications for overall oceanic productivity and
357 carbon cycling.

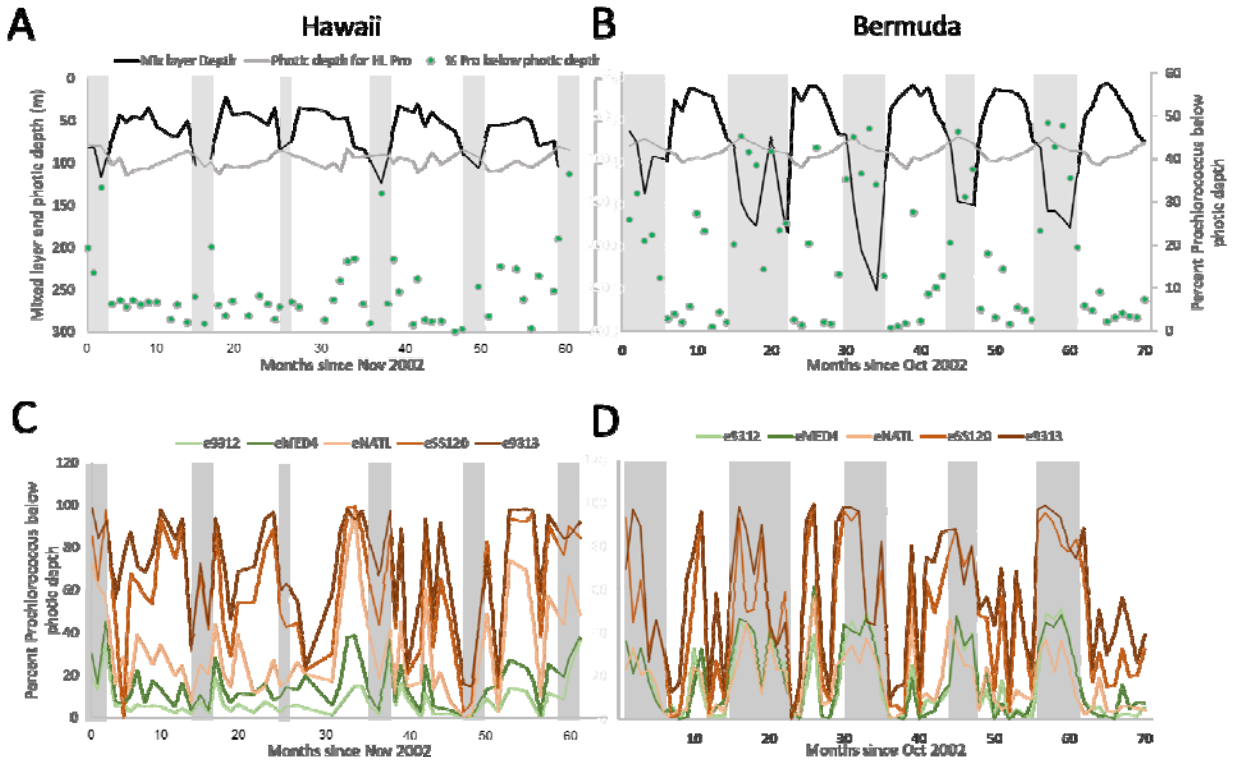

Figure 6: Estimating the number of *Prochlorococcus* cells found below their photic zone at Hawaii and Bermuda. A, B) The percent of total *Prochlorococcus* cells found below their photic zone at Hawaii (A) and Bermuda (B), defined as the integrated illumination level supporting the growth of representative strains in laboratory cultures (50) (grey line shows this depth for HL strains). The black line shows the mixed layer depth (MLD), the grey areas are non-stratified conditions where cells may be mixed from

depth to the surface. C, D) The percentage of each *Prochlorococcus* ecotype below its photic depth. For more information see supplementary text. The data are taken from (49).

358

359

360 **Material and Methods**

361 ***Prochlorococcus* growth and Stable Isotope Incubations**

362 Axenic *Prochlorococcus* strains were grown in Pro99 media under constant cold while light (27 µE) at
363 22 °C. Axenicity of the strains was tested routinely, as well as before all major experiments, using test
364 media (ProMM, (39)). Additionally, no evidence for contaminating heteroteophic cells was observed in
365 flow cytometry, scanning electron microscopy or when axenic *Prochlorococcus* cultures were used as
366 negative controls for 16S amplicon sequencing. Bulk chlorophyll fluorescence (FL) (ex440; em680) was
367 measured almost daily using a Fluorescence Spectrophotometer (Cary Eclipse, Varian). In
368 parallel, samples for flow cytometry were taken for cell numbers. When three distinct sub-populations
369 appeared in the flow cytometry, the cultures were labeled with 1mM Sodium bicarbonate-^{13}C and 1mM
370 Ammonium-^{15}N chloride (Sigma-Aldrich, USA) for 18-24 hours. The optimal incubation time based on
371 preliminary isotope labeling experiments with *Prochlorococcus* MED4, showing that uptake is identified
372 already after 3 hours and is linear until 24 hours under our growth conditions (Supplementary figure 11).
373 Incubations were stopped by fixing 2 ml of the culture with 2X EM grade glutaraldehyde (2.5% final
374 concentration, Sigma) and subsequently storing at 4 °C until the sorting analysis. Non-labeled cells that
375 were killed before labeling (by adding 2.5% glutaraldehyde) were used as a negative control.

376

377 **Cell Sorting and Filtration**

378 Sorting of sub-population was carried out using a BD FACSAria III sorter (BD Biosciences) at the Life
379 Sciences and Engineering Infrastructure Center, Technion, Israel. Each sample was sorted for 3 sub-
380 populations: Non-chlorotic (High-fl), Semi chlorotic (Mid-fl) and Chlorotic (Low-fl) (Figure 2A). The
381 sorting gates for each sub-population were determined from the population observed in forward scatter
382 (FSC, a proxy for cell size) and auto-fluorescence (PerCP, chlorophyll auto-fluorescence). After sorting,
383 the sorted sup-population were gently filtered on 13 mm diameter polycarbonate filters (GTTP, 0.2 µM
384 pore size, Millipore, MA), washed twice with sterile sea water and air-dried. The filters were stored at
385 4°C until nanoSIMS analyses.
386
387 **Nanoscale secondary ion mass spectrometry (nanoSIMS) and data analysis**
388 The samples were coated with a layer of ca. 30 nm gold with a Cressington 108 auto sputter coater
389 (Watford, United Kingdom). Random spots were employed for NanoSIMS analyses. SIMS imaging was
390 performed using a NanoSIMS 50L instrument (Cameca, Paris, France) at the Leibniz-Institute for Baltic
391 Sea Research Warnemünde (IOW). A $^{133}Cs^{+}$ primary ion beam was used to erode and ionize atoms of the
392 sample. Images of secondary electrons, $^{12}C^{-}$, $^{13}C^{-}$, $^{12}C^{14}N^{-}$ and $^{12}C^{15}N^{-}$ were recorded simultaneously using
393 mass detectors equipped with electron multipliers (Hamamatsu). The mass resolving power was
394 adjusted to be sufficient to suppress interferences at all masses allowing, e.g. the separation of $^{13}C^{-}$ from
395 interfering ions such as $^{12}C^{1}H^{-}$. Prior to the analysis, sample areas of 50×50 µm were sputtered for 2 min
396 with 600 pA to erode the gold, clean the surface and reach the steady state of secondary ion formation.
397 The primary ion beam current during the analysis was 1 pA; the scanning parameters were 512×512
398 pixels for areas of 30x30 to 48x48 µm, with a dwell time of 250 µs per pixel. 60 planes were analysed.
399
400 **Analyses of NanoSIMS measurements**

401 All NanoSIMS measurements were analysed with the Matlab based program look@nanosims (73).
402 Briefly, the 60 measured planes were checked for inconsistencies and all usable planes accumulated,
403 regions of interest (ROI's) (i.e. *Prochlorococcus* cells and filter regions without organic material for
404 background measurements) defined based on $^{12}C^{14}N$ mass pictures, and $^{13}C/^{12}C$ as well as $^{12}C^{15}N/^{12}C^{14}N$
405 ratios calculated from the ion signals for each region of interest.

406 **Uptake rate calculation**

407 Uptake rate was estimated using the following equation, based on that of (74), as follows:

$$V = \frac{\left(\%P_t \ - \%P_0\ \right)}{\left(\%D_i \ - \%D_0\ \right)} \frac{Q}{t}$$

408 Where $\%P^*_t$ is the concentration (atom %) of the heavy isotope in the particulate matter at the end of
409 the incubation, $\%D^*_i$ is the concentration of the dissolved tracer added to the incubation (and assumed
410 not to change over the short incubation time), and $\%P^*_0$ and $\%D^*_0$ are the natural heavy isotope
411 concentrations in the particulate and dissolved matter, respectively. We estimated Q, the cell quota (in
412 fg cell^{-1}) of C or N, based on measurements of the biomass of MED4 and MIT9313 (66 fg cell^{-1}and 158 fg
413 cell^{-1}, respectively, (75)) and assuming that C comprises 50% and N comprises 7.5% of the cell biomass.
414 For heavy isotopes concentration in the particulate and dissolved phases before incubation we used the
415 natural values for isotopic ratios of ^{13}C and ^{15}N (1.12% and 0.37% respectively). For the experiment
416 shown in Supplementary Fig. 8, we measured the NH_4^+ concentration in the media and added the ^{15}N
417 tracer to 50% final concentration. Since all other experiments were performed in declining cultures we
418 assumed that the NH_4^+ was depleted from the media, and thus $\%D^*_t$ was defined as 90%, based on
419 previous measurements of NH_4^+ concentrations in old cultures. We used a value of 50% for the initial
420 percentage of ^{13}C, based on dissolved inorganic carbon (DIC) measurements (41). For the terminal
421 concentrations of ^{15}N and ^{13}C in the particulate phase ($\%P^*_t$) we used the values of $^{13}C/^{12}C$ and $^{15}N/^{14}N$

422 that were obtained from the NanoSims analysis of the cells. $^{13}C/^{12}C$ and $^{15}N/^{14}N$ below the natural values
423 resulted with negative uptake values, and were treated as zero uptake.

424 Mean and standard deviation of C and N uptake rates were calculated from the uptake rate values of
425 individual cells (Table 1). The uptake rate values were not corrected for negative control (killed cells),
426 which are presented for comparison in table 1. Since $^{13}C/^{12}C$ and $^{15}N/^{14}N$ values of individual cells were
427 not normally distributed, for significance analysis we used non-parametric tests (Mann-Whitney and
428 Kruskal-Wallis tests) performed using the Real Statistics Resource Pack software (Release 5.4 www.real-
429 statistics.com).

430 **Isotope labelling and phylogenetic analysis of a natural marine bacterioplankton population at sea**
431 **Water collection and labelling experiment procedure**

432 Mediterranean seawater was collected during August 2017 (station N1200, 32.45 degrees N, 34.37
433 degrees E) from 11 depths by Niskin bottles and divided into triplicates of 250 ml polycarbonate bottles.
434 Two bottles from each depth were labeled with 1mM Sodium bicarbonate-^{13}C and 1mM Ammonium-^{15}N
435 chloride (Sigma-Aldrich, USA) and all 3 bottles (2 labelled and 1 control) were incubated at the original
436 depth and station at sea for 3.5 hours on day time. The short incubation time was chosen to minimize
437 isotope dilution and potential recycling and transfer of ^{13}C and ^{15}N between community members (32).
438 After incubation, bottles were brought back on board and the incubations were stopped by fixing with
439 2X EM grade glutaraldehyde (2.5% final concentration) and stored at 4°C until sorting analysis.
440

441 **DNA collection and extraction from seawater**

442 Samples for DNA collected on a 0.22 µm Sterivex filters (Millipore). Excess water was removed using a
443 syringe and 1 ml Lysis buffer (40 mM EDTA, 50 mM Tris pH 8.3, 0.75 M sucrose) was added and both
444 ends were closed with parafilm. Samples were kept at -80°C until extraction. DNA extracted by using a

445 semi-automated protocol includes manually chemical cell lysis before the automated steps. The manual
446 protocol began with thawing the samples, then the storage buffer was removed using a syringe and 170
447 µl lysis buffer added to the filter. 30 µl of Lysozyme (20 mg/ml) added to filters and incubate at 37°C for
448 30 min. After incubation, 20 µl proteinase K and 200 µl Buffer AL added to the tube for 1 hour at 56°C
449 (with agitation). Then, the supernatant transferred to a new tube, which subjected to the QIAcube
450 automated system (at the BioRap unit, Faculty of Medicine, Technion) following the manufacturer's
451 instructions using QIAamp DNA Mini Protocol: DNA Purification from Blood or Body Fluids (Spin
452 Protocol) from step 6. All DNA samples were eluted in 100 µl DNA free distilled-water.
453
454 **16S and ITS PCR amplification**
455 PCR amplification of the ITS was carried out with specific primers for *Prochlorococcus* CS1_16S_1247F
456 (5'-ACACTGACGACATGGTTCTACACGTACTACAATGCTACGG) and Cs2_ITS_Ar (5'-
457 TACGGTAGCAGAGACTTGGTCTGGACCTCACCCTTATCAGGG) (47, 48). The first PCR was performed in
458 triplicate in a total volume of 25 µl containing 0.5 ng of template, 12.5 µl of MyTaq Red Mix (Bioline) and
459 0.5 µl of 10 µM of each primer. The amplification conditions comprised steps at 95°C for 5 min, 28/25
460 (16S/ITS) cycles at 95°C for 30 sec, 50°C for 30 sec and 72°C for 1 min followed by one step of 5 min at
461 72°C. All PCR products validated on 1% agarose gel and triplicates were pooled. Subsequently, a second
462 PCR amplification was performed to prepare libraries. These were pooled and after a quality control
463 sequenced (2x250 paired-end reads) using an Illumina MiSeq sequencer. Library preparation and
464 pooling were performed at the DNA Services (DNAS) facility, Research Resources Center (RRC),
465 University of Illinois at Chicago (UIC). MiSeq sequencing was performed at the W.M. Keck Center for
466 Comparative and Functional Genomics at the University of Illinois at Urbana-Champaign (UIUC).
467

468 **ITS Sequence processing** Paired-end reads, in the format of fastq files were analyzed by the DADA2
469 pipeline (76). Quality of the sequences per sample was examined using the Dada2 'plotQualityProfile'
470 command. Quality filtering was done using the Dada2 'filterAndTrim' command with parameters for
471 quality filtering were truncLen=c(290,260), maxN=0, maxEE=c(2,2), truncQ=2, rm.phix=TRUE,
472 trimLeft=c(20,20). Following error estimation and dereplication, the dada algorithm was used to correct
473 sequences. Merging of the forward and reverse reads was done with minimum overlap of 4 bp.
474 Detection and removal of suspected chimera was done with command 'removeBimeraDenovo'. In total,
475 388,417 sequences in 484 amplicon sequence variants (ASVs) were counted. The ASVs were aligned in
476 MEGA6 (77) and the first ~295 nucleotides, corresponding to the 16S gene, were trimmed. The ITS
477 sequences were then classified using BLAST against a custom database of ITS sequences from cultured
478 *Prochlorococcus* and *Synechococcus* strains as well as from uncultured HL and LL clades.

479

480 **Acknowledgements**

481 We thank the captain and crew of the R/V Mediterranean Explorer and Tom Reich, for help during the
482 work at sea, Maya Lalzar for assistance with the bioinformatics analysis and Annett Grüttmüller for
483 NanoSIMS routine operation. This study was supported by grant RGP0020/2016 from the Human
484 Frontiers Science Program (to MV, HPG and DS) and by grant number 1635070/2016532 from the NSF-
485 BSF program in Oceanography (NSFOCE-BSF, to DS). The NanoSIMS at the Leibnitz-Institute for Baltic Sea
486 research in Warnemuende (IOW) was funded by the German Federal Ministry of Education and
487 Research (BMBF), grant identifier 03F0626A.

488

489 **Author contributions**

490 DRR, DA, TLK, AV, MV and DS designed experiments, DRR, DA, TLK, LZ, NN and DS performed
491 experiments and field analyses, DRR, DA, TLK, AV, and FE performed NanoSIMS analyses, DRR, DA, TLK,
492 AV, LZ, FE, NN, HPG, MV and DS analyzed results, DRR, DA, TLK and DS wrote manuscript with
493 contributions from all authors.
494
495 **Competing interests**
496 The authors declare no competing interests
497
498 **Materials and Correspondence**
499 Please send requests for materials or other correspondence to Daniel Sher, dsher@univ.haifa.ac.il
500
501 **References:**

502 1. Del Giorgio PA, Gasol JM. Physiological Structure and Single-Cell Activity in Marine
503 Bacterioplankton. In: Kirchman DL, editor. Microbial Ecology of the Oceans2008.
504 2. Bergkessel M, Basta DW, Newman DK. The physiology of growth arrest: uniting molecular and
505 environmental microbiology. Nat Rev Microbiol. 2016;14:549.
506 3. Jørgensen BB, Lever MA, Rogers KL, Lloyd KG, Overmann J, Schink B, et al. Life under extreme
507 energy limitation: a synthesis of laboratory- and field-based investigations. FEMS Microbiology Reviews.
508 2015;39(5):688-728.
509 4. Engl C. Noise in bacterial gene expression. Biochemical Society Transactions.
510 2018:BST20180500.
511 5. Harms A, Maisonneuve E, Gerdes K. Mechanisms of bacterial persistence during stress and
512 antibiotic exposure. Science. 2016;354(6318):aaf4268.

513 6. Lennon JT, Jones SE. Microbial seed banks: the ecological and evolutionary implications of
514 dormancy. Nat Rev Microbiol. 2011;9(2):119-30.
515 7. Field CB, Behrenfeld MJ, Randerson JT, Falkowski P. Primary Production of the Biosphere:
516 Integrating Terrestrial and Oceanic Components. Science. 1998;281(5374):237-40.
517 8. Moore CM, Mills MM, Arrigo KR, Berman-Frank I, Bopp L, Boyd PW, et al. Processes and patterns
518 of oceanic nutrient limitation. Nat Geosci. 2013;6(9):701-10.
519 9. Bratbak G, Thingstad TF. Phytoplankton-Bacteria Interactions - an Apparent Paradox - Analysis of
520 a Model System with Both Competition and Commensalism. Mar Ecol-Prog Ser. 1985;25(1):23-30.
521 10. Kirchman DL. Oceanography - Phytoplankton death in the sea. Nature. 1999;398(6725):293-4.
522 11. Franklin DJ, Brussaard CPD, Berges JA. What is the role and nature of programmed cell death in
523 phytoplankton ecology? Eur J Phycol. 2006;41(1):1-14.
524 12. Bidle KD. The Molecular Ecophysiology of Programmed Cell Death in Marine Phytoplankton. Ann
525 Rev Mar Sci. 2015;7(1):341-75.
526 13. Sukenik A, Maldener I, Delhaye T, Viner-Mozzini Y, Sela D, Bormans M. Carbon assimilation and
527 accumulation of cyanophycin during the development of dormant cells (akinetes) in the cyanobacterium
528 Aphanizomenon ovalisporum. Frontiers in Microbiology. 2015;6(1067).
529 14. Sauer J, Schreiber U, Schmid R, Völker U, Forchhammer K. Nitrogen Starvation-Induced Chlorosis
530 in Synechococcus PCC 7942. Low-Level Photosynthesis As a Mechanism of Long-Term Survival. Plant
531 Physiology. 2001;126(1):233-43.
532 15. Klotz A, Georg J, Bučinská L, Watanabe S, Reimann V, Januszewski W, et al. Awakening of a
533 Dormant Cyanobacterium from Nitrogen Chlorosis Reveals a Genetically Determined Program. Current
534 Biology. 2016;26(21):2862-72.

535 16. de Abreu Meireles D, Schripsema J, Vetö Arnholdt AC, Dagnino D. Persistence of Only a Minute
536 Viable Population in Chlorotic Microcystis aeruginosa PCC 7806 Cultures Obtained by Nutrient
537 Limitation. PLOS ONE. 2015;10(7):e0133075.
538 17. Behrenfeld MJ, Falkowski PG. Photosynthetic rates derived from satellite-based chlorophyll
539 concentration. Limnol Oceanogr. 1997;42(1):1-20.
540 18. Veldhuis MJW, Kraay GW, Timmermans KR. Cell death in phytoplankton: correlation between
541 changes in membrane permeability, photosynthetic activity, pigmentation and growth. Eur J Phycol.
542 2001;36(2):167-77.
543 19. Flombaum P, Gallegos JL, Gordillo RA, Rincón J, Zabala LL, Jiao N, et al. Present and future global
544 distributions of the marine Cyanobacteria Prochlorococcus and Synechococcus.
545 Proceedings of the National Academy of Sciences. 2013;110(24):9824-9.
546 20. Ribalet F, Swalwell J, Clayton S, Jiménez V, Sudek S, Lin Y, et al. Light-driven synchrony of
547 Prochlorococcus growth and mortality in the subtropical Pacific gyre. Proceedings of the National
548 Academy of Sciences. 2015;112(26):8008-12.
549 21. Kashtan N, Roggensack SE, Rodrigue S, Thompson JW, Biller SJ, Coe A, et al. Single-Cell Genomics
550 Reveals Hundreds of Coexisting Subpopulations in Wild Prochlorococcus. Science. 2014;344(6182):416-
551 20.
552 22. Martiny AC, Coleman ML, Chisholm SW. Phosphate acquisition genes in Prochlorococcus
553 ecotypes: evidence for genome-wide adaptation. Proc Natl Acad Sci U S A. 2006;103(33):12552-7.
554 23. Berube PM, Rasmussen A, Braakman R, Stepanauskas R, Chisholm SW. Emergence of trait
555 variability through the lens of nitrogen assimilation in Prochlorococcus. eLife. 2019;8:e41043.
556 24. Biller SJ, Berube PM, Lindell D, Chisholm SW. Prochlorococcus: the structure and function of
557 collective diversity. Nat Rev Microbiol. 2014;13:13.

558 25. Steglich C, Behrenfeld M, Koblizek M, Claustre H, Penno S, Prasil O, et al. Nitrogen deprivation
559 strongly affects Photosystem II but not phycoerythrin level in the divinyl-chlorophyll b-containing
560 cyanobacterium Prochlorococcus marinus. Biochimica et Biophysica Acta (BBA) - Bioenergetics.
561 2001;1503(3):341-9.
562 26. Tolonen AC, Aach J, Lindell D, Johnson ZI, Rector T, Steen R, et al. Global gene expression of
563 Prochlorococcus ecotypes in response to changes in nitrogen availability. Mol Syst Biol. 2006;2:53.
564 27. Thompson AW, Huang K, Saito MA, Chisholm SW. Transcriptome response of high- and low-
565 light-adapted Prochlorococcus strains to changing iron availability. Isme J. 2011;5(10):1580-94.
566 28. Krumhardt KM, Callnan K, Roache-Johnson K, Swett T, Robinson D, Reistetter EN, et al. Effects of
567 phosphorus starvation versus limitation on the marine cyanobacterium Prochlorococcus MED4 I: uptake
568 physiology. Environ Microbiol. 2013;15(7):2114-28.
569 29. Domínguez-Martín MA, Gómez-Baena G, Díez J, López-Grueso MJ, Beynon RJ, García-Fernández
570 JM. Quantitative Proteomics Shows Extensive Remodeling Induced by Nitrogen Limitation in <span
571 class="named-content genus-species" id="named-content-1">Prochlorococcus marinus SS120.
572 mSystems. 2017;2(3):e00008-17.
573 30. Coe A, Ghizzoni J, LeGault K, Biller S, Roggensack SE, Chisholm SW. Survival of Prochlorococcus in
574 extended darkness. Limnol Oceanogr. 2016;61(4):1375-88.
575 31. Gao D, Huang X, Tao Y. A critical review of NanoSIMS in analysis of microbial metabolic activities
576 at single-cell level. Critical Reviews in Biotechnology. 2016;36(5):884-90.
577 32. Berthelot H, Duhamel S, L'Helguen S, Maguer J-F, Wang S, Cetinić I, et al. NanoSIMS single cell
578 analyses reveal the contrasting nitrogen sources for small phytoplankton. The ISME Journal. 2018.
579 33. Aharonovich D, Sher D. Transcriptional response of Prochlorococcus to co-culture with a marine
580 Alteromonas: differences between strains and the involvement of putative infochemicals. ISME J.
581 2016;10(12):2892-906.

582 34. Domínguez-Martín MA, López-Lozano A, Clavería-Gimeno R, Velázquez-Campoy A, Seidel G,
583 Burkovski A, et al. Differential NtcA Responsiveness to 2-Oxoglutarate Underlies the Diversity of C/N
584 Balance Regulation in Prochlorococcus. Frontiers in Microbiology. 2018;8(2641).
585 35. Domínguez-Martín MA, López-Lozano A, Rangel-Zúñiga OA, Díez J, García-Fernández JM. Distinct
586 features of C/N balance regulation in Prochlorococcus sp. strain MIT9313. FEMS microbiology letters.
587 2017;365(3).
588 36. Matantseva O, Skarlato S, Vogts A, Pozdnyakov I, Liskow I, Schubert H, et al. Superposition of
589 Individual Activities: Urea-Mediated Suppression of Nitrate Uptake in the Dinoflagellate Prorocentrum
590 minimum Revealed at the Population and Single-Cell Levels. Frontiers in Microbiology. 2016;7(1310).
591 37. Agusti S, Sanchez MC. Cell viability in natural phytoplankton communities quantified by a
592 membrane permeability probe. Limnol Oceanogr. 2002;47(3):818-28.
593 38. Hughes C, Franklin DJ, Malin G. Iodomethane production by two important marine
594 cyanobacteria: Prochlorococcus marinus (CCMP 2389) and Synechococcus sp. (CCMP 2370). Marine
595 Chemistry. 2011;125(1–4):19-25.
596 39. Morris JJ, Kirkegaard R, Szul MJ, Johnson ZI, Zinser ER. Facilitation of robust growth of
597 Prochlorococcus colonies and dilute liquid cultures by "helper" heterotrophic bacteria. Appl Environ
598 Microbiol. 2008;74(14):4530-4.
599 40. Moore LR, Coe A, Zinser ER, Saito MA, Sullivan MB, Lindell D, et al. Culturing the marine
600 cyanobacterium Prochlorococcus. Limnol Oceanog Methods. 2007;5:353-62.
601 41. Grossowicz M, Roth-Rosenberg D, Aharonovich D, Silverman J, Follows MJ, Sher D.
602 Prochlorococcus in the lab and in silico: The importance of representing exudation. Limnol Oceanogr.
603 2017;62(2):818-35.

604 42. Fadeev E, De Pascale F, Vezzi A, Hübner S, Aharonovich D, Sher D. Why close a bacterial
605 genome? The plasmid of Alteromonas macleodii HOT1A3 is a vector for inter-specific transfer of a
606 flexible genomic island. Frontiers in Microbiology. 2016;7.
607 43. Sher D, Thompson JW, Kashtan N, Croal L, Chisholm SW. Response of Prochlorococcus ecotypes
608 to co-culture with diverse marine bacteria. Isme J. 2011;5(7):1125-32.
609 44. Christie-Oleza JA, Sousoni D, Lloyd M, Armengaud J, Scanlan DJ. Nutrient recycling facilitates
610 long-term stability of marine microbial phototroph–heterotroph interactions. Nature Microbiology.
611 2017;2:17100.
612 45. Campbell L, Vaulot D. Photosynthetic picoplankton community structure in the subtropical
613 North Pacific Ocean near Hawaii (station ALOHA). Deep Sea Res I. 1993;40(10):2043-60.
614 46. Moore LR, Rocap G, Chisholm SW. Physiology and molecular phylogeny of coexisting
615 Prochlorococcus ecotypes. Nature. 1998;393(6684):464-7.
616 47. Thompson AW, van den Engh G, Ahlgren NA, Kouba K, Ward S, Wilson ST, et al. Dynamics of
617 Prochlorococcus Diversity and Photoacclimation During Short-Term Shifts in Water Column Stratification
618 at Station ALOHA. Frontiers in Marine Science. 2018;5(488).
619 48. Ahlgren NA, Perelman JN, Yeh Y-C, Fuhrman JA. Multi-year dynamics of fine-scale marine
620 cyanobacterial populations are more strongly explained by phage interactions than abiotic, bottom-up
621 factors. Environ Microbiol. 2019;21(8):2948-63.
622 49. Malmstrom RR, Coe A, Kettler GC, Martiny AC, Frias-Lopez J, Zinser ER, et al. Temporal dynamics
623 of Prochlorococcus ecotypes in the Atlantic and Pacific oceans. Isme J. 2010.
624 50. Moore LR, Chisholm SW. Photophysiology of the marine cyanobacterium Prochlorococcus:
625 Ecotypic differences among cultured isolates. Limnol Oceanogr. 1999;44(3):628-38.

626 51. Goericke R, Welschmeyer NA. The marine prochlorophyte Prochlorococcus contributes
627 significantly to phytoplankton biomass and primary production in the Sargasso Sea. Deep Sea Res I.
628 1993;40(11):2283-94.
629 52. Vaulot D, Marie D, Olson RJ, Chisholm SW. Growth of prochlorococcus, a photosynthetic
630 prokaryote, in the equatorial pacific ocean. Science. 1995;268(5216):1480-2.
631 53. Binder BJ, Chisholm SW, Olson RJ, Frankel SL, Worden AZ. Dynamics of picophytoplankton,
632 ultraphytoplankton and bacteria in the central equatorial Pacific. Deep Sea Res II. 1996;43(4):907-31.
633 54. Partensky F, Blanchot J, Lantoine F, Neveux J, Marie D. Vertical structure of picophytoplankton
634 at different trophic sites of the tropical northeastern Atlantic Ocean. Deep Sea Res I. 1996;43(8):1191-
635 213.
636 55. Ting CS, Rocap G, King J, Chisholm SW. Cyanobacterial photosynthesis in the oceans: the origins
637 and significance of divergent light-harvesting strategies. Trends in Microbiology. 2002;10(3):134-42.
638 56. Lichtlé C, Thomas JC, Spilar A, Partensky F. Immunological and ultrastructural characterization of
639 the photosynthetic complexes of the prochlorophyte Prochlorococcus (Oxychlorobacteria). Journal of
640 Phycology. 1995;31(6):934-41.
641 57. Saito MA, McIlvin MR, Moran DM, Goepfert TJ, DiTullio GR, Post AF, et al. Multiple nutrient
642 stresses at intersecting Pacific Ocean biomes detected by protein biomarkers. Science.
643 2014;345(6201):1173-7.
644 58. Yooseph S, Nealson KH, Rusch DB, McCrow JP, Dupont CL, Kim M, et al. Genomic and functional
645 adaptation in surface ocean planktonic prokaryotes. Nature. 2010;468:60.
646 59. Giovannoni SJ. SAR11 Bacteria: The Most Abundant Plankton in the Oceans. Ann Rev Mar Sci.
647 2017;9(1):231-55.
648 60. Llabrés M, Agustí S, Herndl GJ. Diel in situ picoplankton cell death cycles coupled with cell
649 division. Journal of Phycology. 2011;47(6):1247-57.

650 61. Van Mooy BA, Rocap G, Fredricks HF, Evans CT, Devol AH. Sulfolipids dramatically decrease
651 phosphorus demand by picocyanobacteria in oligotrophic marine environments. Proc Natl Acad Sci U S
652 A. 2006;103(23):8607-12.
653 62. Gilbert JDJ, Fagan WF. Contrasting mechanisms of proteomic nitrogen thrift in Prochlorococcus.
654 Mol Ecol. 2011;20(1):92-104.
655 63. Read RW, Berube PM, Biller SJ, Neveux I, Cubillos-Ruiz A, Chisholm SW, et al. Nitrogen cost
656 minimization is promoted by structural changes in the transcriptome of N-deprived Prochlorococcus
657 cells. The ISME journal. 2017;11(10):2267-78.
658 64. Zubkov MV, Tarran GA, Fuchs BM. Depth related amino acid uptake by Prochlorococcus
659 cyanobacteria in the Southern Atlantic tropical gyre. Fems Microbiol Ecol. 2004;50(3):153-61.
660 65. Muñoz-Marín MdC, Luque I, Zubkov MV, Hill PG, Diez J, García-Fernández JM. Prochlorococcus
661 can use the Pro1404 transporter to take up glucose at nanomolar concentrations in the Atlantic Ocean.
662 Proceedings of the National Academy of Sciences. 2013;110(21):8597-602.
663 66. Vila-Costa M, Simó R, Harada H, Gasol JM, Slezak D, Kiene RP. Dimethylsulfoniopropionate
664 Uptake by Marine Phytoplankton. Science. 2006;314(5799):652-4.
665 67. Becker JW, Hogle SL, Rosendo K, Chisholm SW. Co-culture and biogeography of Prochlorococcus
666 and SAR11. The ISME Journal. 2019.
667 68. Rocap G, Larimer FW, Lamerdin J, Malfatti S, Chain P, Ahlgren NA, et al. Genome divergence in
668 two Prochlorococcus ecotypes reflects oceanic niche differentiation. Nature. 2003;424(6952):1042-7.
669 69. Yelton AP, Acinas SG, Sunagawa S, Bork P, Pedrós-Alió C, Chisholm SW. Global genetic capacity
670 for mixotrophy in marine picocyanobacteria. The Isme Journal. 2016;10:2946.
671 70. Morris JJ, Lenski RE, Zinser ER. The Black Queen Hypothesis: Evolution of Dependencies through
672 Adaptive Gene Loss. mBio. 2012;3(2).

673 71. Ma L, Calfee BC, Morris JJ, Johnson ZI, Zinser ER. Degradation of hydrogen peroxide at the
674 ocean's surface: the influence of the microbial community on the realized thermal niche of
675 Prochlorococcus. The Isme Journal. 2017;12:473.
676 72. Hennon GMM, Morris JJ, Haley ST, Zinser ER, Durrant AR, Entwistle E, et al. The impact of
677 elevated CO2 on Prochlorococcus and microbial interactions with 'helper' bacterium Alteromonas. The
678 Isme Journal. 2017;12:520.
679 73. Polerecky L, Adam B, Milucka J, Musat N, Vagner T, Kuypers MM. Look@NanoSIMS--a tool for
680 the analysis of nanoSIMS data in environmental microbiology. Environ Microbiol. 2012;14(4):1009-23.
681 74. Legendre L, Gosselin M. Estimation of N or C uptake rates by phytoplankton using 15N or 13C:
682 revisiting the usual computation formulae. J Plankt Res. 1997;19(2):263-71.
683 75. Cermak N, Becker JW, Knudsen SM, Chisholm SW, Manalis SR, Polz MF. Direct single-cell
684 biomass estimates for marine bacteria via Archimedes' principle. The Isme Journal. 2016;11:825.
685 76. Callahan BJ, McMurdie PJ, Rosen MJ, Han AW, Johnson AJA, Holmes SP. DADA2: High-resolution
686 sample inference from Illumina amplicon data. Nature Methods. 2016;13:581.
687 77. Tamura K, Stecher G, Peterson D, Filipski A, Kumar S. MEGA6: Molecular Evolutionary Genetics
688 Analysis Version 6.0. Molecular Biology and Evolution. 2013;30(12):2725-9.

689